Electronic Supplementary Material (ESI) for Catalysis Science & Technology.

Supplementary information for

Entrapment of a pyridine derivative within copper-palladium alloy: a bifunctional catalyst for electrochemical reduction of CO_2 to alcohols with excellent selectivity and reusability

Heng-Pan Yang, Sen Qin, Ying-Na Yue, Li Liu, Huan Wang* and Jia-Xing Lu**

Shanghai Key Laboratory of Green Chemistry and Chemical Processes, School of Chemistry and Molecular Engineering, East China Normal University, Shanghai 200062, China.
**Corresponding Author: Dr. Huan Wang (Tel: +8621-52134935, E-mail: hwang@chem.ecnu.edu.cn).*
***Corresponding Author: Prof. Jia-Xing Lu (Tel: +8621-62233491, E-mail: jxlu@chem.ecnu.edu.cn).*

1. Materials and Instruments

All reagents except for PYD were used as received.

The synthesis and characterization of PYD were described in reference 14.

Potentiostatic electrolysis and linear sweep voltammograms were performed using a CHI 660C electrochemical Station (Shanghai Chenhua Instruments Company).

^{13}C-NMR spectra were recorded on an Ascend 400 (400 MHz, Bruker, Germany) spectrometer in $CDCl_3$ with Me_4Si as an internal standard.

Liquid phase products were quantitative analyzed by Gas Chromatography-Flame Ionization Detector (GC-FID) (SHIMADZU, GC-2014C).

The dopant amount in filtrate were determined by a high performance liquid chromatography (HPLC) instrument (DIONEX Ultimate 3000 pump) equipped with a UV (RS Variable Wavelength) detector.

Microstructure and EDX mapping were analyzed using Hitachi S-4800 field emission Scanning Electron Microscope (FE-SEM) equipped with an energy dispersive X-ray fluorescence spectrometer (EDX, Oxford; UK).

TEM patterns were recorded by TECNAI G2F30 Transmission Electron Microscope.

X-ray diffraction (XRD) patterns were recorded by a Ultima IV X-ray powder diffractometer using Cu Kα radiation (k= 1.5406 Å).

2. General methods

Synthesis of [PYD]@Cu-Pd: For entrapment of PYD to produce [PYD]@Cu-Pd, a 50 mL water solution of 0.9 g of sodium dodecyl sulphate, 24 mg PYD, 0.52 g $CuCl_2 \cdot 2H_2O$ and 0.56 g $PdCl_2$ was stirred at 550 rpm for a few minutes, until all reagents were fully dissolved. Then 0.5 g of zinc powder was added to the solution, and the combined slurry was stirred for another 6 hours. The precipitate, [PYD]@Cu–Pd, was filtered and washed with 10 mL HCl 1 M to remove zinc residues and metal salts, followed by another wash with 20 mL distilled water for three times and then dried under vacuum for 6 hours. Fine and dark powder was achieved after filtration and drying.

Synthesis of Cu-Pd alloy: Cu-Pd alloy was prepared in the same way except for the absence of PYD in reducing solution. Fine and dark powder was achieved after filtration and drying (Fig. S1).

Synthesis of [PYD]@Cu: A solution of 0.85 g of $CuCl_2$ in 25 mL of distilled water was poured into a stirred solution of 0.6 g of sodium dodecyl sulphate and 9 mg PYD in 25 mL of H_2O. After 5 min of stirring, 0.35 g of zinc powder was added and the combined slurry was stirred at room temperature for 6 h. The precipitate, [PYD]@Cu, was filtered and washed with 10 mL HCl 1 M to remove zinc residues and metal salts, followed by another wash with 20 mL distilled water for three times and then dried under vacuum for 6 hours. The color and shine of the powder is like typical copper (Fig. S2).

Synthesis of pure Cu NPs: pure Cu NPs (Fig. S3) was prepared in the same way except for the absence of $PdCl_2$ and PYD in reducing solution.

Synthesis of [PYD]@Pd: The synthesis and characterization of [PYD]@Pd were described in reference 17.

Synthesis of pure Pd NPs: The synthesis and characterization of pure Pd NPs were described in reference 17.

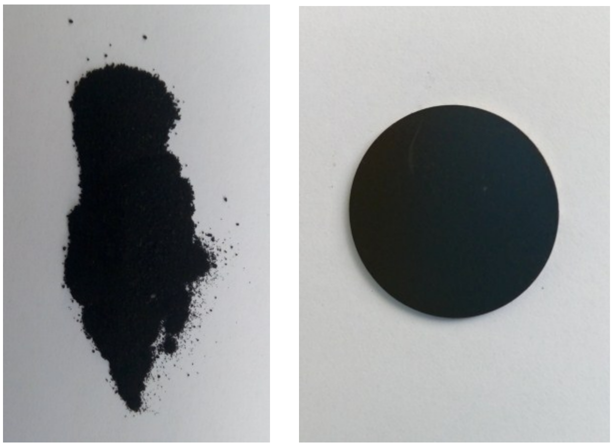

Fig. S1 Cu-Pd alloy before (left) and after (right) press.

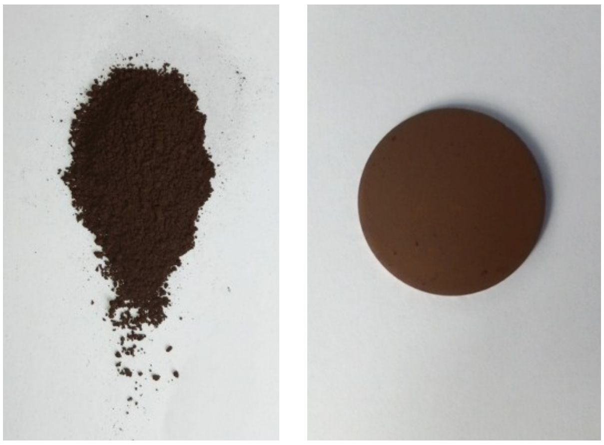

Fig. S2 [PYD]@Cu before (left) and after (right) press.

Fig. S3 Pure Cu NPs before (left) and after (right) press.

Potentiostatic CO_2 reduction procedure: Powder of [PYD]@Cu-Pd (or other powder) was compacted into coin （D= 2 cm，Fig. 1）and used as cathode to test the catalytic activity for CO_2 electroreduction. It was performed with a conventional three-electrode electrochemical H-type cell, in which a piece of Nafion®117 membrane was used as a separator. A saturated calomel electrode (SCE) saturated with KCl was the reference electrode, and a Pt foil (99.999% purity, 10 mm × 10 mm) was the counter electrode. An aqueous electrolyte of 10 mL 0.5 M KCl was used as electrolyte, which was bubbled with 1.0 atm CO_2 (99.995%) to be saturated with CO_2. The pH was preserved at 5.4. The potential was -0.04 V or –0.64 V vs. RHE, and charge used was 50 C.

Linear sweep voltammograms were recorded in an undivided cell. A saturated calomel electrode (SCE) saturated with KCl was the reference electrode, and a Pt foil (99.999% purity, 10 mm × 10 mm) was the counter electrode. An aqueous electrolyte of 10 mL 0.5 M KCl was used as electrolyte, which was bubbled with 1.0 atm N_2 or CO_2 (99.995%). The pH was preserved at 5.4. Scan rate was 0.1 V s^{-1}.

3. Characterization of pure [PYD]@Cu-Pd, Cu-Pd alloy, Cu NPs, and [PYD]@Cu.

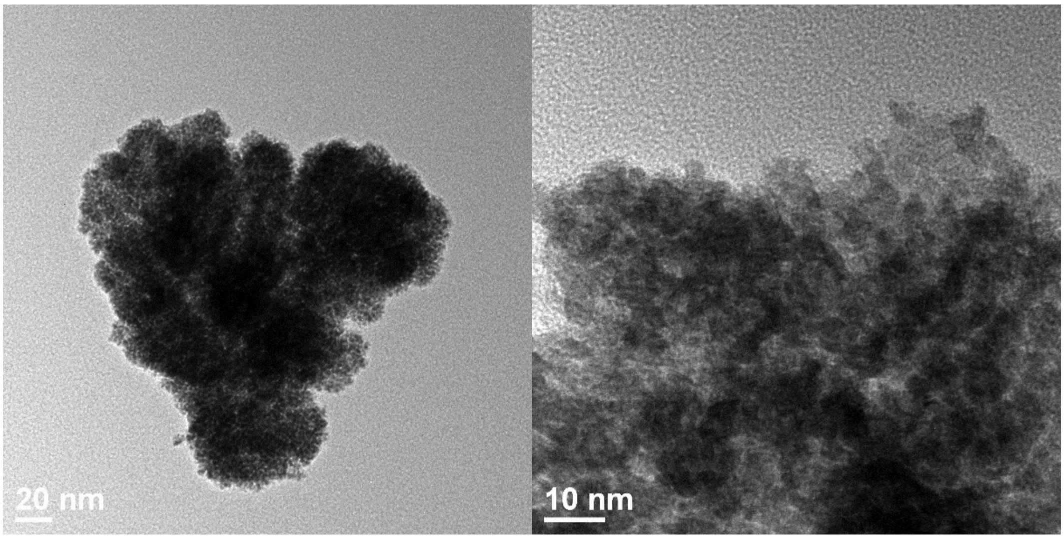

Fig. S4 TEM patterns of [PYD]@Cu-Pd with different scale bars, left (20 nm), right (10 nm).

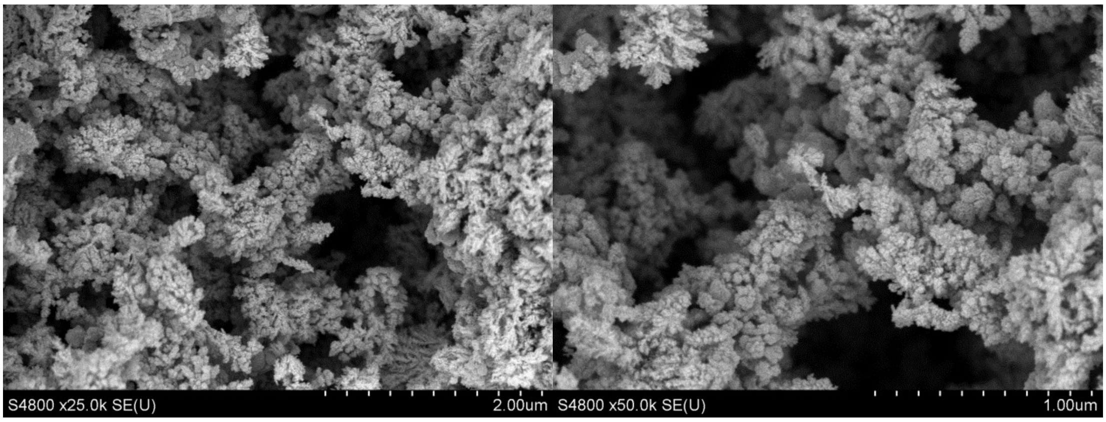

Fig. S5 FE-SEM patterns of pure Cu-Pd alloy with different magnification, left (25k), right (50k).

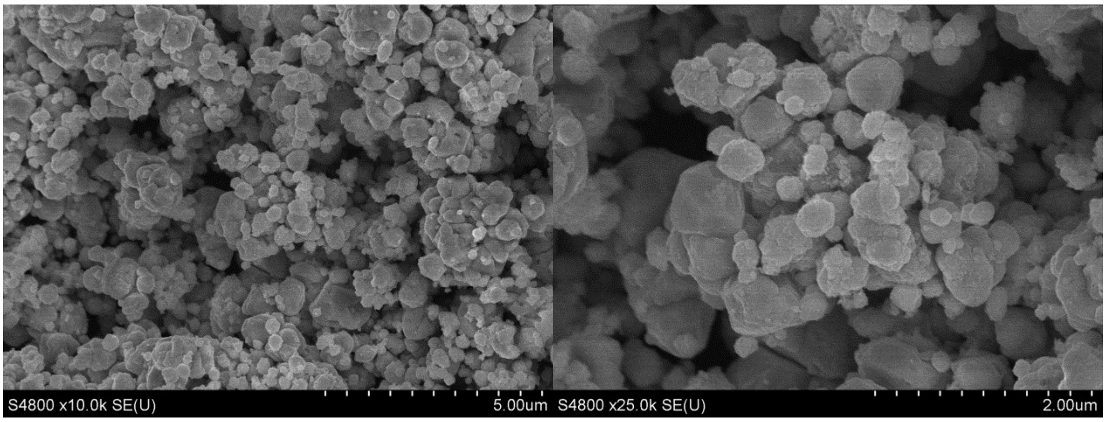

Fig. S6 FE-SEM patterns of pure Cu NPs with different magnification, left (10k), right (25k).

Fig. S7 FE-SEM patterns of [PYD]@Cu (up) with different magnification, left (10k), right (25k);

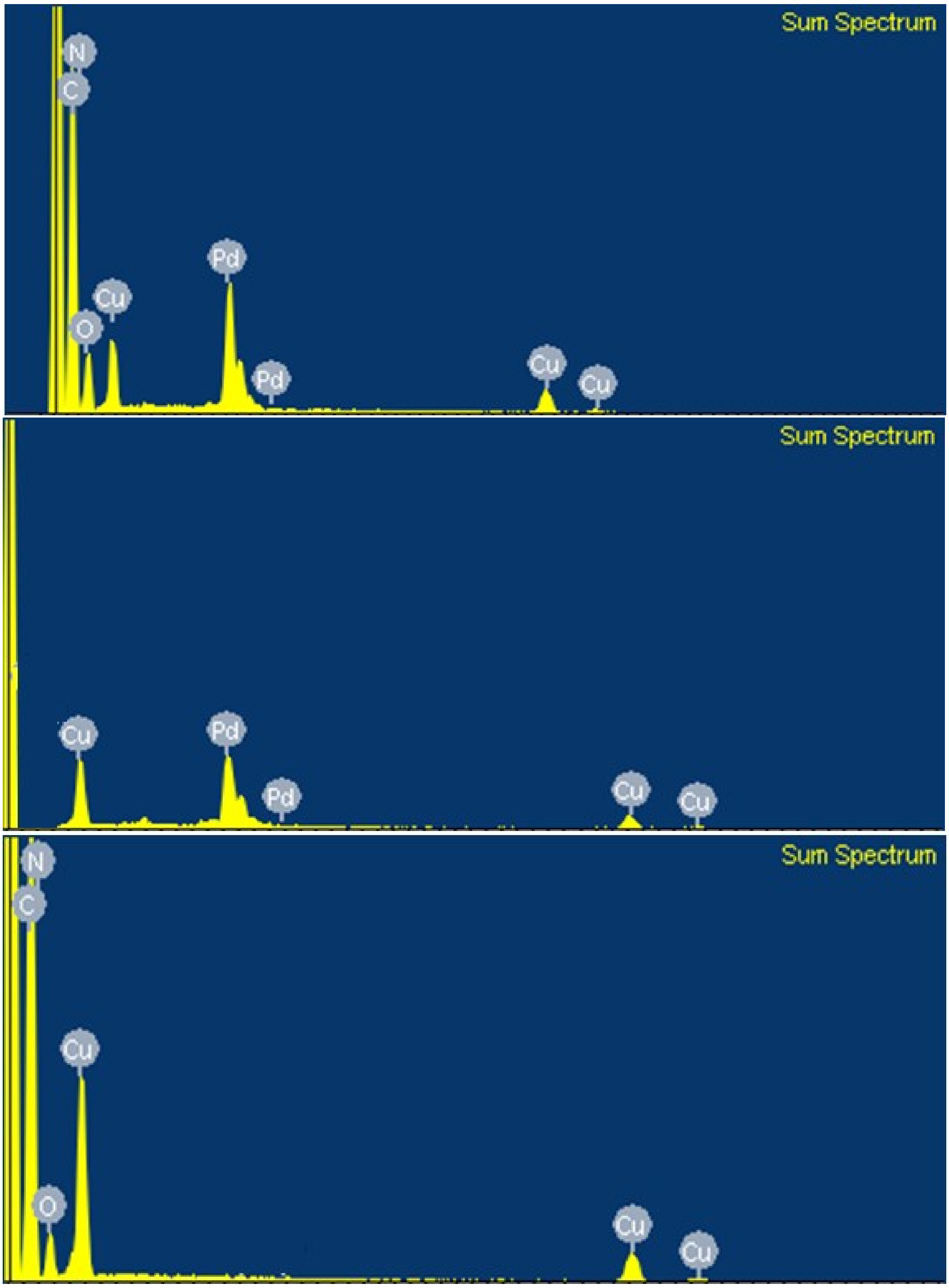

Fig. S8 The EDX spectrum of [PYD]@Cu-Pd (up), Cu-Pd alloy (middle) and [PYD]@Cu (down).

4. Difference between entrapment and adsorption

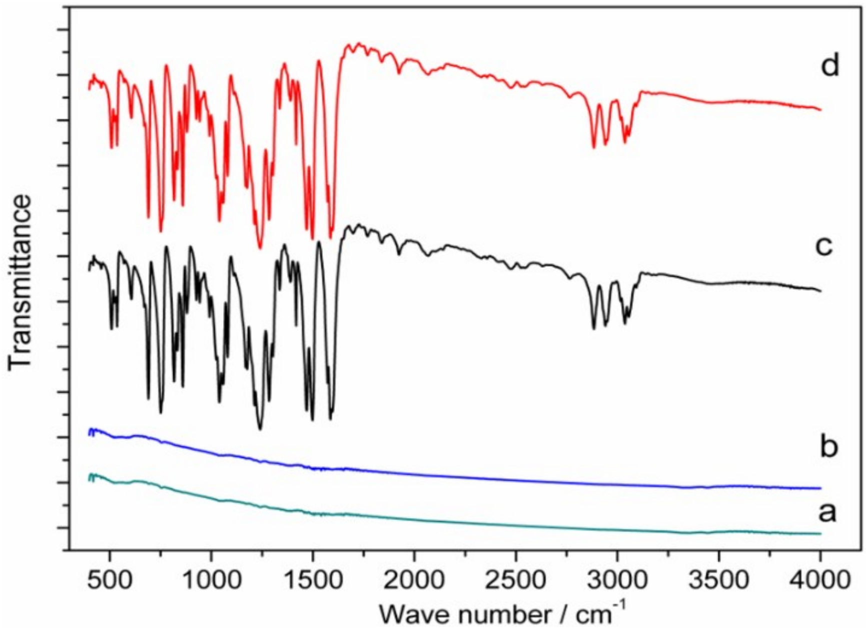

Fig. S9 FT-IR spectra of [PYD]@Cu-Pd (a), pure PYD (c), Cu-Pd alloy after physical adsorption (d), (d) after washed with MeCN (b)

.

Fourier transformed infrared (FT-IR) could further explore the difference between entrapment and adsorption. After physical adsorption in PYD solution, FT-IR spectra of Cu-Pd alloy (Fig. S9d) was almost identical to pure PYD (Fig. S9c). In [PYD]@Cu-Pd composite, PYD could not be detected by FT-IR spectra (Fig. S9a), but the presence of dopant could be confirmed by other characterization methods, like XRD. If (d) was washed with MeCN, there was also no trace of PYD in FT-IR spectra (b), indicating that this adsorption is unstable. In summary, entrapment was fundamentally different from adsorption and much more stable.

5. Characterization of products

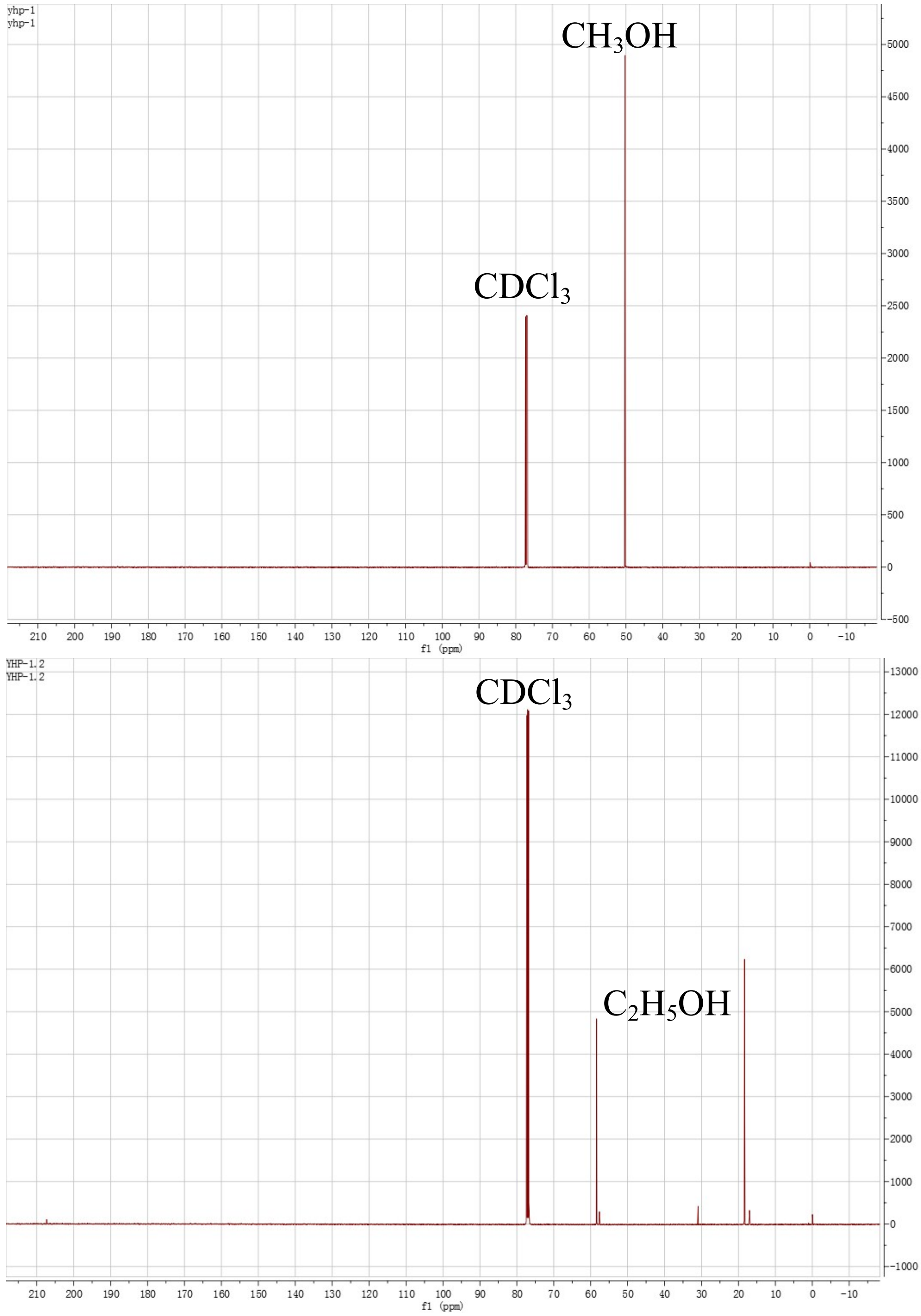

Fig. S10 ^{13}C spectrum of products obtained at [PYD]@Cu-Pd with -0.04 V (up) and -0.64 V vs RHE (down) cathode potential.

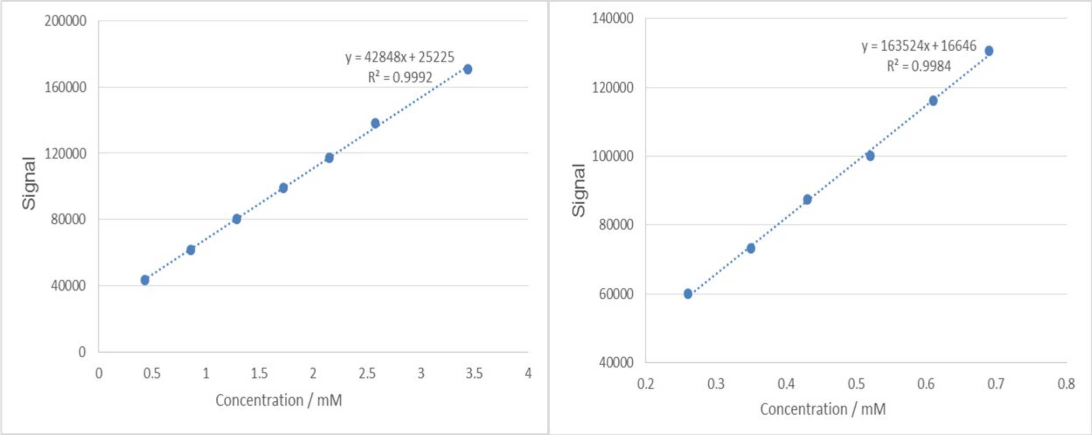

Fig. S11 Calibration curves of methanol (left) and ethanol (right) detected by gas chromatography.

6. LSV at pure Pd NPs electrode.

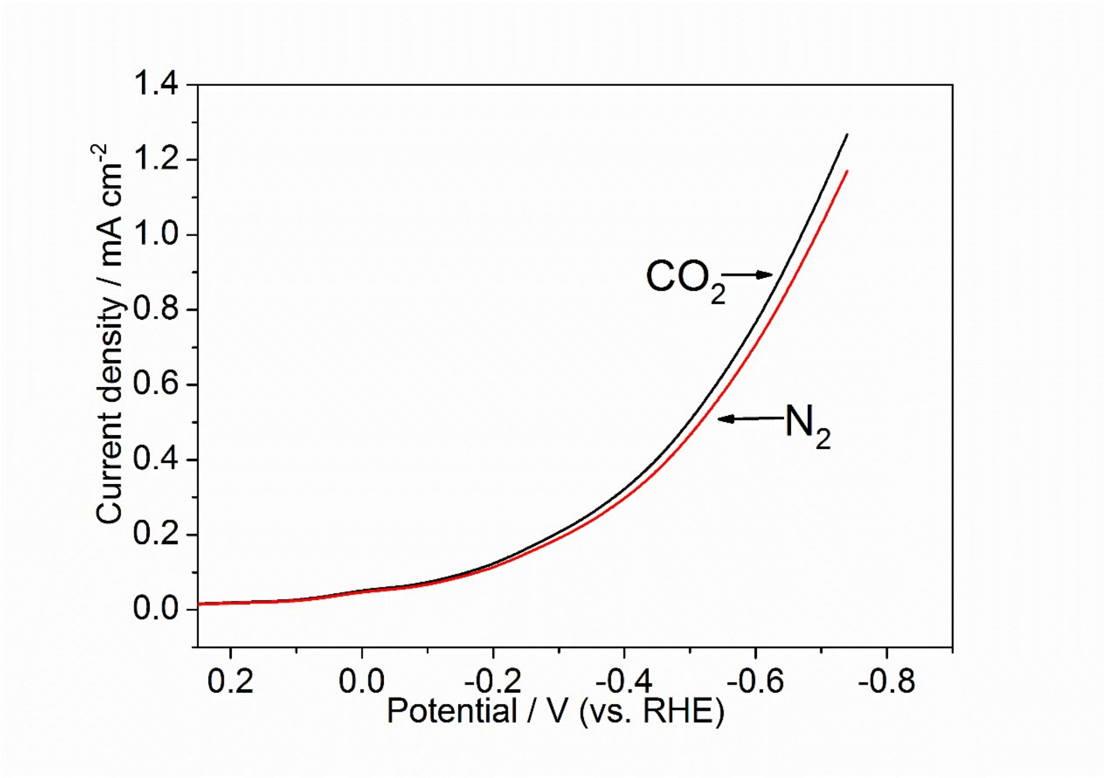

Fig. S12 Linear sweep voltammograms recorded at a sweep rate of 0.1 V s^{-1} in 10 mL 0.5 M KCl solution at pure Pd NPs electrode.

7. Characterization of [PYD]@Cu-Pd after reuse.

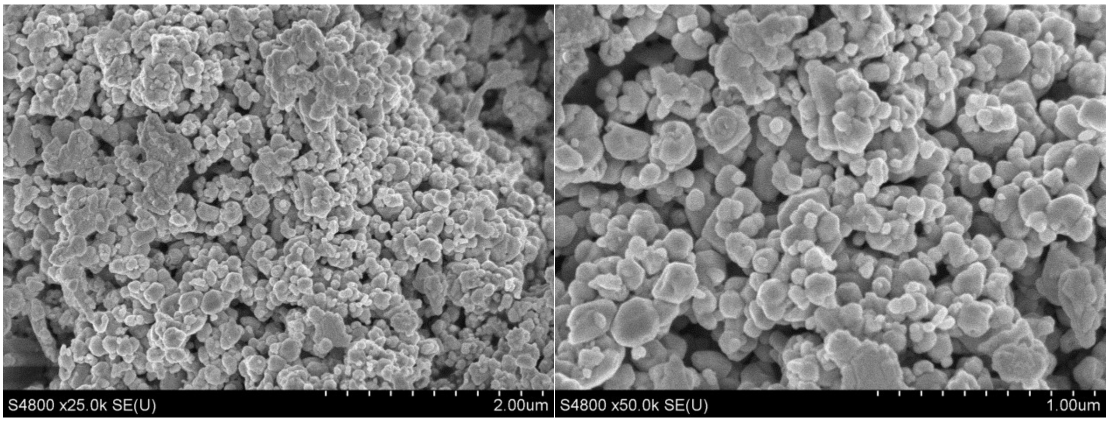

Fig. S13 FE-SEM patterns of [PYD]@Cu-Pd after long test and reuse with different magnification, left (25k), right (50k).

According to SEM patterns, [PYD]@Cu-Pd remained its porous structure after reuse.

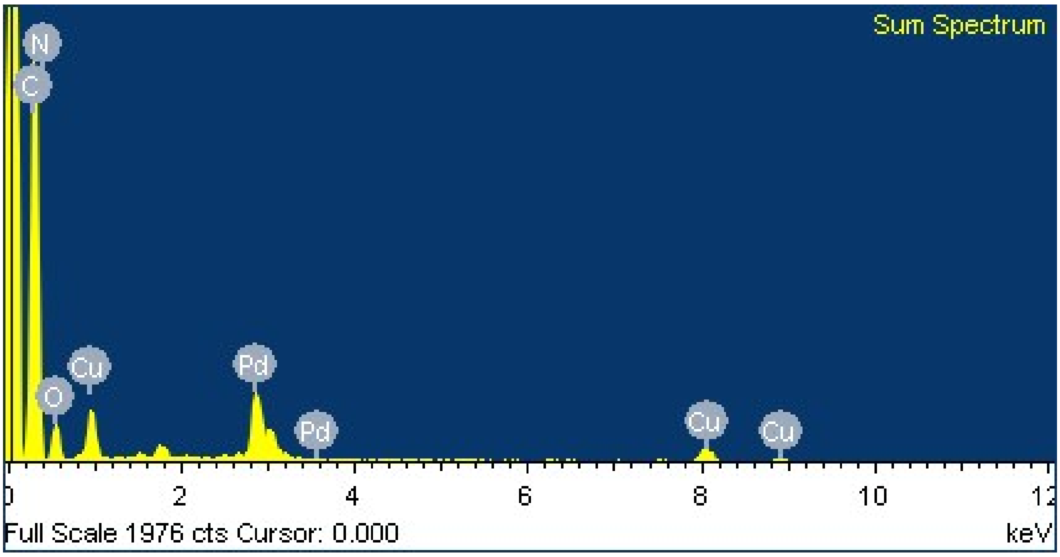

Fig. S14 EDAX patterns of [PYD]@Cu-Pd after reuse show signals corresponding to copper, palladium, nitrogen, carbon and oxygen.